ADVANCED FUNCTIONAL MATERIALS
www.afm-journal.de

Cation–Anion Interaction-Directed Molecular Design Strategy for Mechanochromic Luminescence

*Gaocan Li, Feijie Song, Di Wu, Jingbo Lan, Xingyan Liu, Jie Wu, Shuaijun Yang, Dan Xiao, and Jingsong You**

Mechanofluorochromic materials have great potential for a wide variety of applications such as sensors, memory devices, motion systems, security systems, and so forth. However, only few design principles have been disclosed, which greatly impedes the growth of mechanofluorochromic dyes. Here, a strategy of molecular design for mechanochromic luminescence is reported, based on the cation–anion interaction-directed switching of molecular stacking. On the basis of this strategy, a series of common N-heteroaromatic onium fluorophores such as imidazolium, 1,2,4-triazolium, triazolopyridinium, benzoimidazolium, γ-carbolinium, and pyridinium salts have been designed and proved to have striking reversible mechanofluorochromic behaviors. The simple attachment of a non-fluorescent imidazolium unit to the pyrene scaffold through a flexible carbon chain can even trigger the mechanofluorochromic phenomenon, which gives a consummate interpretation that the cation–anion interaction can be considered as an important general tool to design organic mechanochromic luminescent materials.

1. Introduction

Mechanochromic luminescent materials, as a kind of "smart" stimuli-responsive materials, have great potential for various applications such as sensors, memory devices, motion systems, security systems, and so forth.[1,2] Although many cases have been reported in the literature, the understanding of the relationship between molecular structures and mechano-responsive behaviors still remains obscure. Up to now, only few examples demonstrate the rational molecular designs of mechanochromic luminescence.[2] Such hurdles have greatly impeded the growth of mechanofluorochromic dyes. In particular, the number of mechanical-stimuli-responsive organic small molecule materials is still limited despite the popularity of organic fluorophores.[1,2] Currently, mechanically induced luminescence changes have been observed mainly in certain metal (Au, Cu, Ag, Zn, Pt, Al, and Pd)[3–9] and boron complexes,[10] anthracene and pyrene-based molecules,[11–14] oligo(*p*-phenylene vinylene) derivatives,[15,16] and others.[17–21] Undoubtedly, it is highly desirable, yet very challenging, to establish fundamental principles of molecular design that can be applied to assemble a large number of libraries of mechanofluorochromic dyes.

Mechanochromic materials commonly rely on the changes in physical molecular packing modes.[1,2] From this perspective, mechanochromic phenomenon is ascribed to a reversible switching between two different stable or metastable mechano-dependent molecular stacking models in the solid state. Generally, molecular stacking may be controllable by various secondary intermolecular interactions. Metal-metal interaction, π–π interaction, hydrogen bonding and dipole-dipole interaction have been proposed as possible parameters to trigger an alteration of the stacking modes.[1] However, the cation–anion interaction, an important type of interaction, has been almost entirely ignored for the rational design of organic mechanochromic luminescent materials.

To enable a reproducible switching of mechano-dependent molecular stacking modes, a subtle balance of diverse intra- and intermolecular interactions appears to represent a crucial prerequisite.[1,11,15] It is well-known that the cation–anion interaction is one of the important interactions to govern the molecular packing modes of onium salts and, thus, can lead to changes in the properties such as melting point, density, viscosity, and electrical conductivity.[22–25] Given that the molecular assemblies of organic cations with a rich set of anions can offer a great abundance of cation-anion interactions, we envisioned that the cation-anion interactions and other intra- and intermolecular interactions could be regarded as ideal competing factors to reach such a balance through the variation of counteranions. Thus, onium salts would be promising candidates for mechanochromic luminescent materials.

Another important requirement to achieve these goals mentioned above is that the organic cation exhibits significant luminescent properties in the solid state. Imidazolium salts have been shown to be the most common type of ionic liquids (ILs), typically bearing two alkyl groups at the two nitrogen atoms of the imidazolium core. Unfortunately, these imidazolium salts

G. Li, Dr. F. Song, Prof. Dr. D. Wu, Prof. Dr. J. Lan, X. Liu, J. Wu, Dr. S. Yang, Prof. Dr. D. Xiao, Prof. Dr. J. You
Key Laboratory of Green Chemistry and Technology of Ministry of Education
College of Chemistry
and State Key Laboratory of Biotherapy
West China Medical School
Sichuan University
29 Wangjiang Road, Chengdu, 610064, PR China
E-mail: jsyou@scu.edu.cn

DOI: 10.1002/adfm.201302086

© 2013 WILEY-VCH Verlag GmbH & Co. KGaA, Weinheim

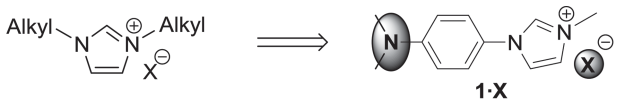

Scheme 1. Molecular modification of imidazolium salts.

generally exhibit very low emission intensities in the visible region ($\Phi_f < 0.05$) probably due to their relatively small chromophores.[26] Consequently, it becomes difficult to observe the mechanofluorochromic phenomenon. Recently, a new generation of aryl alkyl ionic liquids (TAAILs) containing alkyl and aryl substituents at the nitrogen atoms has been developed.[27] Their physicochemical and electronic properties may be tuned by altering anions or substituents at the nitrogen atoms. Herein, we disclose that the modular modification of the phenylimidazolium core can offer minimal fluorophores that not only emit intense visible light in the solid state, but also exhibit reversible mechanochromic luminescence through a simple adjustment of anion (**Scheme 1**).

2. Results and Discussion

2.1. Influence of Anions on Mechanochromic Luminescence

The phenylimidazolium salts, as a parent core, do not show luminescence emission in the visible region. Considering that the electron-deficient imidazolium ring is the electron-accepting moiety, the proper introduction of an electron donor such as dialkylamino on the benzene ring would present a "push–pull" π-electron mode, offering an unlocking opportunity for visible photoluminescence. The synthesis of aryl alkyl imidazolium salts with different counteranions included the copper-catalyzed *N*-arylation of imidazoles, followed by the quaternization of the imidazole ring at the N3-position with alkyl halide, and subsequent anion exchange.[28] The initially prepared imidazolium salt **1·I** with an iodine anion displayed very weak fluorescence ($\Phi_f = 0.002$) in the solid state, which was presumably attributed to the external heavy atom effect of a halogen atom. After surveying a series of common counteranions such as NTf_2^- (bis((trifluoromethyl)sulfonyl)amide), PF_6^-, OTf^-, BF_4^- and $N(CN)_2^-$, the NTf_2^- anion was proven to be an ideal counteranion to enable excellent luminescent properties (**Table 1**). Moreover, the emission wavelengths varied with different counteranions, which implied that different molecular packing modes could be gained by tuning anions.

Owing to the low emission quantum yield of **1·I** in the solid state, we chose five counteranions (i.e., NTf_2^-, PF_6^-, OTf^-, BF_4^-, and $N(CN)_2^-$) to illustrate the correlation between the cation–anion interaction and the mechanochromic performance of **1·X** (X = counteranion). After three minutes of pressing under 6 MPa using an oil press, **1·NTf$_2$**, **1·PF$_6$**, **1·OTf**, **1·BF$_4$**, and **1·N(CN)$_2$** underwent redshifts of the peak emission wavelengths (approximately 102 nm, 90 nm, 78 nm, 36 nm, and 7 nm, respectively) (Table 1 and **Figure 1**a), which was in good agreement with the known order of the strength of the cation-anion interaction as following: $NTf_2^- < PF_4^- < OTf^- < BF_4^- < N(CN)_2^-$.[22–25] It hinted that the strength of the cation-anion interaction could determine the mechanochromic luminescence property to a certain extent. The NTf_2^- anion associated with the delocalization of negative charge and the shielding effect of the sulfonyl oxygens and trifluoromethane groups is widely used to reduce the capacity of the cation-anion interaction to develop low melting ionic liquids.[29] In this context, the NTf_2^- anion was well demonstrated as an ideal counteranion to induce mechanochromic luminescence. We rationalized that the weak interactions between the imidazolium cation and the NTf_2^- anion made molecular stacking relatively loose. The loose molecular stacking was more susceptible to tiny slip by mechanical stimuli. It is worth noting that **1·NTf$_2$** is one of the smallest fluorophore exhibiting an obvious mechanofluorochromic behavior, which constitutes one of the longest emission wavelength redshifts reported so far.[2,14]

2.2. Mechanochromic Luminescence of 1·NTf$_2$

To gain further understanding of the mechanochromic performance, the influence of applied pressure on the mechanochromic luminescence of **1·NTf$_2$** was investigated. As the operating pressure increased from 0 to 6 MPa, a gradual redshift of the fluorescence emission of the **1·NTf$_2$** powder appeared with a peak wavelength change from 407 nm to 509 nm (Figure 1b), which implied that different stress conditions could lead to the tiny dissimilarity in the molecular aggregation. However, after the pressure exceeded 6 MPa, no further redshifts of the emission wavelengths were observed.

Table 1. Physical and photophysical properties of onium salts **1·X**.

1·X	M.p. [°C]	λ_{abs} [nm][a] (in $CHCl_3$)	λ_{em} (nm)[b] (Φ_f)[c] (pristine)	λ_{em} (nm)[b] (under 6.0 MPa pressure)	Emission wavelength shift [nm]
1·NTf$_2$	82-83	299	407 (0.76)	509	102
1·PF$_6$	133-134	299	371 (0.12)	461	90
1·OTf	58-60	300	423 (0.59)	501	78
1·BF$_4$	156-157	302	433 (0.45)	469	36
1·N(CN)$_2$	108-110	298	418 (0.53)	425	7

[a]Only the wavelengths of maximum absorption are shown; [b]Excited at 370 nm (excited at 350 nm for **1·PF$_6$**); [c]Absolute emission quantum yields estimated by calibrated integrating sphere system.

© 2013 WILEY-VCH Verlag GmbH & Co. KGaA, Weinheim

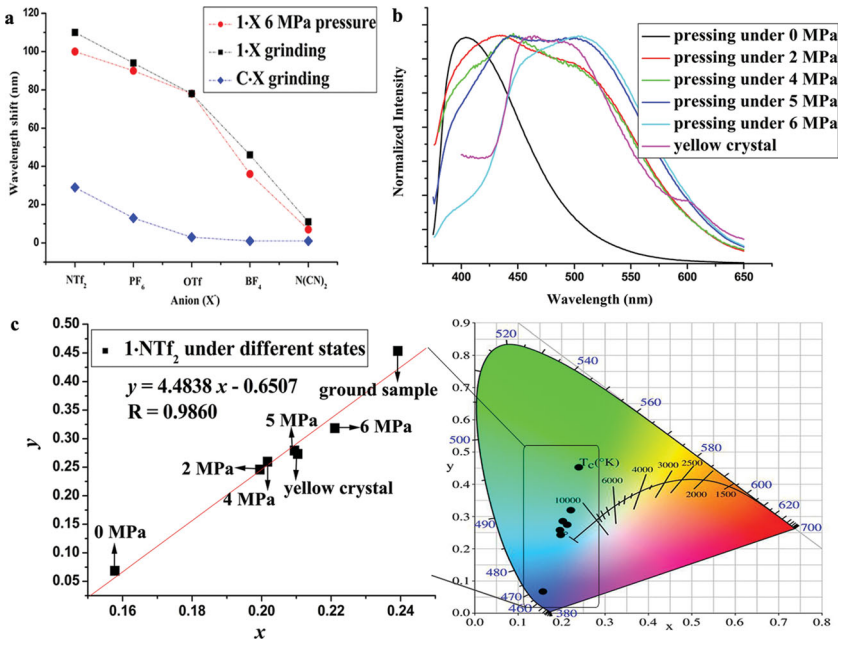

Figure 1. a) Mechanochromic performance of onium salts **1·X** and **C·X** with different counteranions upon grinding and under pressure (3 min, 6 MPa). b) Normalized emission spectra of the powder under the external pressure and yellow crystals of **1·NTf$_2$** excited at 370 nm. c) Chromaticity analysis of **1·NTf$_2$** in different states shown in (a,b): a linear trajectory of chromaticity coordinates plotted on a 1931 CIE diagram.

The imidazolium salt **1·NTf$_2$** is a white crystalline powder as prepared and displayed a blue emission (λ_{em} = 407 nm) with a fluorescence quantum yield (Φ_f = 0.76) in the solid state (**Figure 2**a,b,n). After being heated to the melting state and cooled down to room temperature, the pristine white powder switched to a pale yellow solid emitting a yellowish-green luminescence (λ_{em} = 518 nm, Φ_f = 0.25), which could remain for several months at room temperature (Figure 2c,d,n). Upon a gentle grinding with a spatula, the blue emission was converted to the yellowish-green luminescence (Figure 2e,f,n). Figure 1a,c clearly indicated that the grinding process exhibited a more redshifted light emission than the pressing operation (111 nm versus 102 nm), which hinted that these two different operations might have different effect on molecular packing or conformation variations. As illustrated in the confocal laser-scanning microscopy (CFLSM) images, even a tiny scratch on the surface of colorless crystals also resulted in a yellow emission color (as the emission below 500 nm was filtered out) under irradiation at 405 nm (Figure 2j–m). The perturbed yellowish-green-emitting

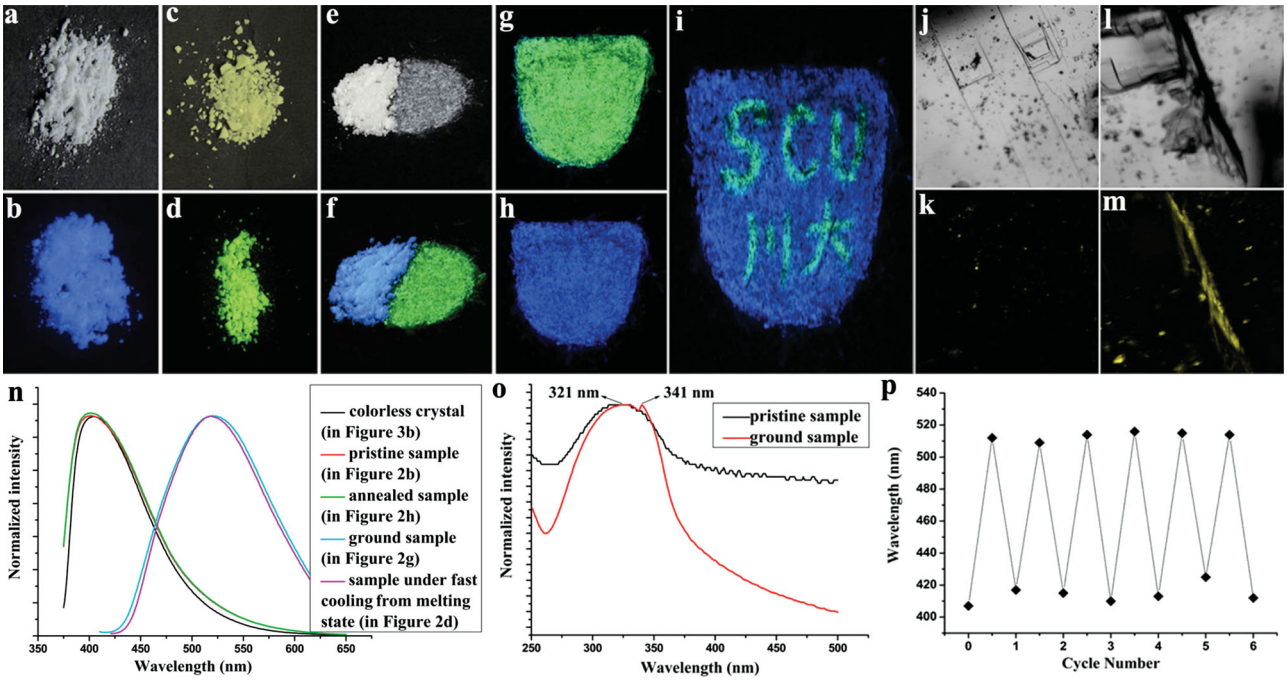

Figure 2. Photographs of **1·NTf$_2$** under ambient light and UV irradiation at 365 nm: a) the pristine crystalline powder under ambient light, and b) under UV light; c) the solid under fast cooling from its melting state under ambient light, and d) under UV light; e) the pristine solid after grinding the right-half with a spatula under ambient light, and f) under UV light; g) the entirely ground solid, and h) the sample after thermal annealing under UV light; and i) the regeneration of the yellowish-green emission demonstrated by the letters "SCU" and the Chinese characters "Sichuan University" written with a spatula. CFLSM images of colorless single crystal of **1·NTf$_2$**: j) the image of unscratched crystal under ambient light, and k) under irradiation at 405 nm; and l) the image of crystal with a tiny scratch under ambient light, and m) under irradiation at 405 nm (as the emission below 500 nm was filtered out). n) Normalized emission spectra of **1·NTf$_2$** in different states excited at 370 nm. o) Normalized UV-visible absorption spectra of **1·NTf$_2$** in thin film before and after grinding. p) Reversible switching of emission of **1·NTf$_2$** by repeated grinding-heating cycles (λ_{ex} = 370 nm).

© 2013 WILEY-VCH Verlag GmbH & Co. KGaA, Weinheim

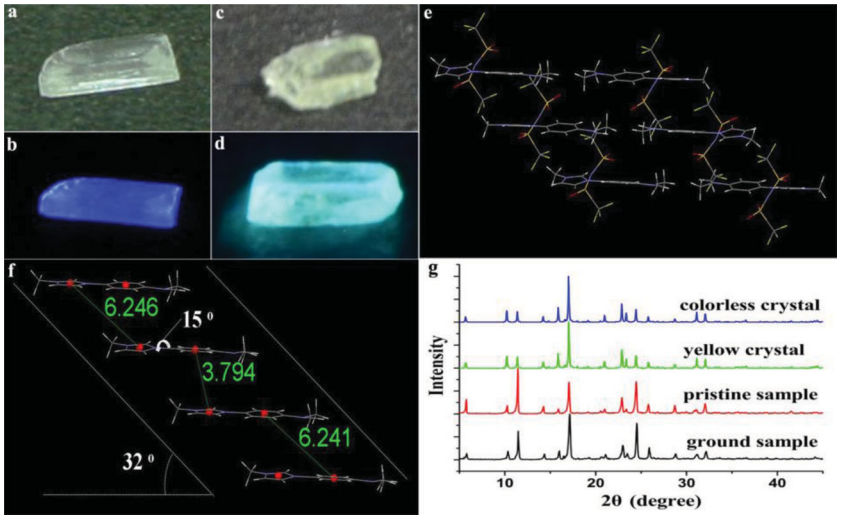

Figure 3. Photographs of single crystals of **1·NTf$_2$**: a) the colorless single crystal under ambient light, and b) under UV light (λ_{ex} = 365 nm); and c) the yellow single crystal under ambient light, and d) under UV light (λ_{ex} = 365 nm). Molecular stacking of the colorless single crystals of **1·NTf$_2$**: e) side view; and f) partial view of the crystal packing with anions omitted for clarity. g) Powder X-ray diffraction patterns of **1·NTf$_2$** in different states.

sample was treated with thermal annealing at approximately 80 °C to revert back to the blue emission (Figure 2g,h,n), and recovered again by subsequent regrinding (Figure 2i). The emission of **1·NTf$_2$** could be reversibly switched between the two different phases by repeated grinding and annealing treatments with no obvious fatigue response (Figure 2p).

2.3. Investigation of Plausible Mechanism of Piezochromic Luminescence of 1·NTf$_2$

To gain insight into the mechanism of piezochromic luminescence of **1·NTf$_2$**, both single crystal X-ray diffraction (XRD) and powder X-ray diffraction (PXRD) measurements were conducted. After numerous attempts, two different forms of crystals of **1 NTf$_2$** were fortunately isolated from the dilute and concentrated ethyl acetate solutions in refrigerator, respectively (**Figure 3**a–d). X-ray single crystal structural analysis of the colorless crystals revealed that the molecules stacked in a face-to-face orientation with a slip angle of approximately 32° along the long molecular axis, and a dihedral angle of approximately 15° between the phenyl ring and the imidazolium ring (Figure 3e,f). Furthermore, only weak π–π interactions in the sheet-like stacking pattern were observed through analysis with the program PLATON. Interestingly, the yellow crystals did exhibit the stacking pattern and the cell parameters identical to the colorless ones (Supporting Information, Figures S3,S4, and Table S2). Although the XRD patterns of the pristine powder agreed well with those simulated from the single crystal data in both crystalline forms, the diffraction data of the ground solid showed tiny changes in the diffraction peaks, which disclosed the possible formation of new aggregates (Figure 3g and Figure S5, Supporting Information). The colorless crystals displayed blue emission very similar to the emission spectra of the pristine powder and the annealed sample with the emission wavelength of about 407 nm (Figures 3b, 2n). The yellow ones emitted blue-green fluorescence, which was neither consistent with the ground sample nor the pristine powder (Figures 3d, 2n, 1b). Therefore, one could suggest that the mechanism was differentfrom the well-known typical models, in which obvious changes in the XRD patterns are observed.[1,2]

Subsequently, absorption and fluorescence decay measurements of the pristine and ground samples of **1·NTf$_2$** were carried out. The absorption spectra clearly showed a new small absorption peak at a longer wavelength of 341 nm after grinding (Figure 2o), which suggested the generation of a new aggregate during the grinding process. The phenomena could also be explained by the different fluorescence emissions and lifetimes of the white pristine powder (λ_{em} = 407 nm, τ = 3.5 ns) and the yellowish ground sample (λ_{em} = 518 nm, τ = 4.2 ns) (Figure S6, Supporting Information). Furthermore, chromaticity analysis of **1·NTf$_2$** illustrated that the samples in different states were probably binary blends of the blue-emitting aggregate (absorption at 321 nm) and the new aggregate (absorption at 341 nm) (Figure 1c, 2o). The concentration of the new aggregate in the yellow crystals was too low to be detected by single crystal XRD measurements. Differential scanning calorimetry (DSC) analysis for the pristine and ground samples of **1·NTf$_2$** showed that the ground sample generated a new, very small endothermic peak at approximately 71 °C before melting in the first heating curve (**Figure 4**), which further suggested the formation of new aggregate with a low concentration.[13] However, despite very small amounts of the new aggregate, its luminescence efficiency reached a high enough level to cause the pronounced change in fluorescence emission.[3] We assumed that a tiny slip of the molecular stacking after grinding or pressure led to the generation of new aggregates ascribed to the local distortions in the whole crystalline structure or the formation of the local amorphous

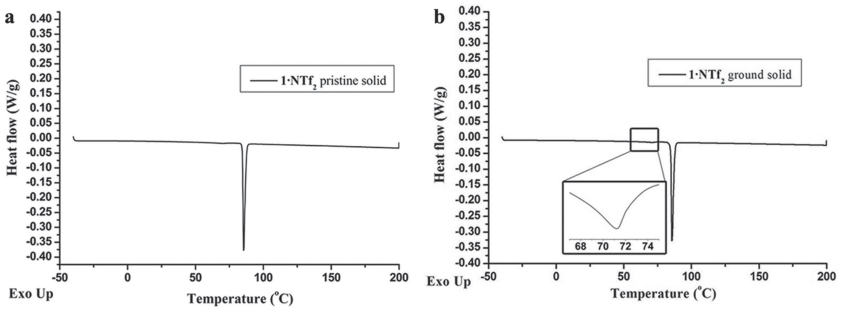

Figure 4. DSC curves (first heating) of **1·NTf$_2$** in different states: a) pristine solid and b) ground solid.

© 2013 WILEY-VCH Verlag GmbH & Co. KGaA, Weinheim

Table 2. Physical and photophysical properties of onium salts **1·NTf$_2$**-**8·NTf$_2$**.

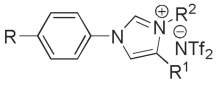

1·NTf$_2$ R = dimethylamino, R^1 = H, R^2 = Me
2·NTf$_2$ R = dimethylamino, R^1 = H, R^2 = Et
3·NTf$_2$ R = butylmethylamino, R^1 = H, R^2 = Me
4·NTf$_2$ R = diethylamino, R^1 = H, R^2 = Me
5·NTf$_2$ R = piperidin-1-yl, R^1 = H, R^2 = Me
6·NTf$_2$ R = dimethylamino, R^1 = Me, R^2 = Et
7·NTf$_2$ R = dimethylamino, R^1 = COOEt, R^2 = Me
8·NTf$_2$ R = dimethylamino, R^1 = 4-CNPh, R^2 = Me

Compd.	M.p. [°C][a)]	λ_{abs} [nm][b)] (in $CHCl_3$)	λ_{em} [nm][c)] (Φ_f)[d)] (pristine)	λ_{em} [nm][c)] (ground)	Emission wavelength shift [nm]
1·NTf$_2$	86	299	407 (0.76)	518	111
2·NTf$_2$	–[e)]	293	479 (0.05)	–	–
3·NTf$_2$	–[e)]	302	481 (0.03)	–	–
4·NTf$_2$	–[e)]	307	484 (0.10)	–	–
5·NTf$_2$	70	290	430 (0.45)	472	42
6·NTf$_2$	86	289	414 (0.45)	504	90
7·NTf$_2$	80	299	425 (0.38)	492	67
8·NTf$_2$	122	253	453 (0.13)	532	79

[a)]Melting points were obtained from the first heating run using DSC under N_2, rate = 5 °C min^{-1}; [b)]Only the maximum absorption wavelengths are shown; [c)]Emission of samples excited at the corresponding maximum excitation wavelength; [d)]Absolute emission quantum yields estimated by calibrated integrating sphere system; [e)]Room temperature ionic liquid.

state with the enhancement of aromatic stacking interactions or dipole-dipole interaction, which resulted in a red-shifted emission. In addition, other aspects such as molecular conformation variation after grinding or pressure might also have great effect on luminescence of fluorophore. Upon grinding or enhancing the external pressure, an increase in the amount of the new aggregates induced a gradual redshift of the emission wavelength from 407 nm to 518 nm (Figure 1b,c). Upon thermal annealing treatment, the metastable new aggregate was recovered to the more stable blue-emitting aggregate.

2.4. Application of Molecular Design Strategy

This molecular design strategy is simple, yet capable of developing a broad range of onium materials showing piezochromic luminescence. For example, the aryl alkyl imidazolium-based salts **1·NTf$_2$**-**8·NTf$_2$** with the NTf$_2^-$ counteranion were modularly synthesized through judicious choice of the substituents of the "phenylimidazolium" parent core (**Table 2**). The alkyl chain length of the substituents (even one more carbon atom in the chain) could drastically influence the melting point of imidazolium salts. When the methyl substituent in **1·NTf$_2$** was replaced by the ethyl group, the room temperature ionic liquid **2·NTf$_2$** was obtained. Compounds **3·NTf$_2$** and **4·NTf$_2$** bearing the butylmethylamino and diethylamino substituents on the phenyl ring respectively were also ionic liquids. The imidazolium salt with a more electron-donating substituent on the phenyl ring (**5·NTf$_2$**) and the salts with electron-withdrawing substituents on the imidazolium ring (**7·NTf$_2$**, and **8·NTf$_2$**) emitted redshifted fluorescence compared with **1·NTf$_2$**. Except ionic liquids **2·NTf$_2$**, **3·NTf$_2$** and **4·NTf$_2$**, all the prepared imidazolium salts exhibited significant reversible mechanochromic luminescence with various emission wavelength redshifts (42–111 nm). It demonstrated that the modification of the parent phenylimidazolium fluorephore core could influence the cation-anion interactions and thus resulted in the different mechanochromic properties of these imidazolium salts.

To further test our hypothesis, we designed and synthesized a series of other *N*-heteroaromatic onium fluorophores such as [1,2,4]triazolo[4,3-*a*]pyridin-2-ium salts (**Pz·X**), benzoimidazol-3-ium salts (**Bz·X**), γ-carbolinium salts (**C·X**), and pyridinium salts (**Py·X**). As expected, these common organic onium salts were found to display significant mechanofluorochromic behaviors through a choice of suitable anion (**Table 3** and Table S1, Supporting Information). Similar to imidazolium salts, other azolium salts such as [1,2,4]triazolo[4,3-*a*]pyridin-2-ium salts (**Pz·NTf$_2$**) and benzoimidazol-3-ium salts (**Bz·NTf$_2$**) exhibited approximately 40 nm emission wavelength redshifts after grinding. The emission of the pyridinium salt **Py·NTf$_2$** was redshifted from 648 nm to 712 nm (the near infrared region) after grinding. Notably, the mechanochromic performance of **C·X** (X: NTf$_2^-$, PF$_6^-$, OTf$^-$, BF$_4^-$, and N(CN)$_2^-$) was also in accordance with the order of the strength of the cation-anion interaction (Figure 1a). Upon thermal annealing or recrystallization, the ground samples of these onium salts were easily recovered to the original state. As known, no obvious mechanochromic luminescence was observed for the fluorescent pyrene. However, the simple attachment of a non-fluorescent imidazolium unit to the pyrene scaffold through a flexible carbon chain (**P·X**) could induce the reversible mechanochromic luminescence, which demonstrated that the cation–anion interaction could be considered as a general strategy in designing organic mechanochromic luminescent materials.

3. Conclusions

We have established the cation-anion interaction-directed strategy for the rational design of mechanochromic

© 2013 WILEY-VCH Verlag GmbH & Co. KGaA, Weinheim

Table 3. Physical and photophysical properties of onium salts.

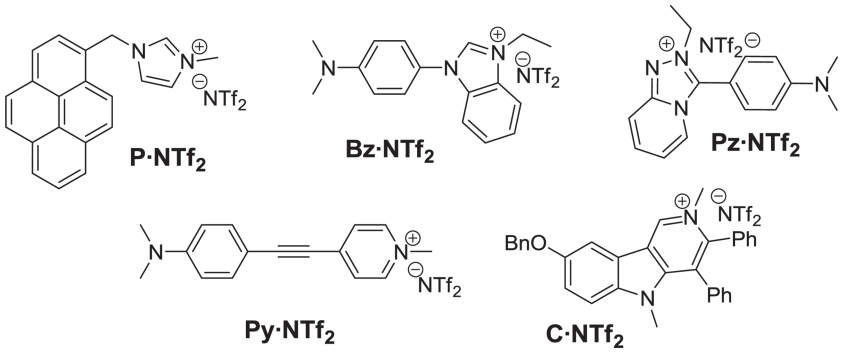

Compd.	M.p. [°C]	λ_{abs} [nm][a] (in $CHCl_3$)	λ_{em} [nm][b] (Φ_f)[c] (pristine)	λ_{em} [nm][b] (ground)	Emission wavelength shift [nm]
P·NTf$_2$	59-61	375	415 (0.07)	486	71
Bz·NTf$_2$	65-68	316	475 (0.55)	511	36
Pz·NTf$_2$	92-93	345	434 (0.06)	472	38
Py·NTf$_2$	146-147	478	648 (0.09)	712	64
C·NTf$_2$	163-164	338	456 (0.23)	485	29

[a]Only the maximum absorption wavelengths are shown; [b]Excited at the corresponding maximum excitation wavelength; [c]Absolute emission quantum yields estimated by calibrated integrating sphere system.

luminescence. This strategy has been successfully harnessed to discover a wide range of onium piezochromic luminescent materials such as imidazolium salts, 1,2,4-triazolium salts, triazolopyridinium salts, benzoimidazolium salts, γ-carbolinium salts, and pyridinium salts. The possible mechanism of piezochromic luminescence of **1·NTf$_2$** has been proposed, but each onium salt itself may have an idiographic model. Although a deeper understanding of the relationship between molecular structures and mechano-responsive behaviors is still required, these first results have already opened a new avenue of investigation into stimuli-responsive luminescent materials, and may enable organic onium salts to find an array of novel applications in sensors, memory devices, liquid crystals, optical displays, and rewritable optical media.

4. Experimental Section

Instrumentation: NMR spectra were obtained on a Bruker AV II-400 or Bruker AV II-600. Fluorescence emission spectra were obtained using a Horiba Jobin Yvon-Edison Fluoromax-4 fluorescence spectrometer. Absorption spectra were obtained on a HITACHI U-2910 spectrometer. Fluorescence lifetime data were determined in 1 mm cell on a Hamamatsu FL920S instrument. Differential scanning calorimetry (DSC) data was performed using a TA instrument DSC-Q200 1474 (rate = 5 °C min^{-1}, range = –40 to 200 °C). The ESI-TOF mass spectra were recorded with a Waters Q-Tof premier instrument. X-Ray single-crystal diffraction data were collected on an Oxford Xcalibur E CCD area-detector diffractometer. Melting points were determined with XRC-1 and are uncorrected.

General Procedure for the Synthesis of Neutral N-Arylheterocycles: A flame-dried Schlenk tube with a magnetic stir bar was charged with aryl iodide (5.0 mmol), free (*N*–H) heterocycle (6.0 mmol), CuI (0.380 g, 1.0 mmol), base (10.0 mmol) and DMF (5.0 mL) under N_2. The reaction system was then evacuated and backfilled with N_2 for twice. After stirring at the indicated temperature for 36 h, DMF was removed under reduced pressure and the residue was purified by column chromatography on silica gel.

General Procedure for the Synthesis of Onium Salts: A Schlenk tube with a magnetic stir bar was charged with neutral N-arylheterocycles, alkyl halide and solvent under N_2. The resulting mixture was stirred at indicated temperature for 24 h and the solvent was then removed. The residue was purified by column chromatography on silica gel and the product was further purified by recrystallization.

Crystallographic data for the structures reported in this paper have been deposited with the Cambridge Crystallographic Data Centre as supplementary publication no. CCDC-912422 and no. CCDC-912423 for colorless crystal and yellow crystal of **1·NTf$_2$**, respectively.

Supporting Information

Supporting Information is available from the Wiley Online Library or from the author.

Acknowledgements

This work was supported the National High Technology Research and Development Program of China (863 Program) (No. 2013AA031901) and the National NSF of China (Nos 21025205, 21272160, and 21021001).

Received: June 19, 2013
Revised: August 20, 2013
Published online: September 3, 2013

[1] Y. Sagara, T. Kato, *Nat. Chem.* **2009**, *1*, 605.
[2] Z. Chi, X. Zhang, B. Xu, X. Zhou, C. Ma, Y. Zhang, S. Liu, J. Xu, *Chem. Soc. Rev.* **2012**, *41*, 3878.

© 2013 WILEY-VCH Verlag GmbH & Co. KGaA, Weinheim

[3] S. Perruchas, X. F. L. Goff, S. Maron, I. Maurin, F. Guillen, A. Garcia, T. Gacoin, J.-P. Boilot, *J. Am. Chem. Soc.* **2010**, *132*, 10967.
[4] H. Ito, T. Saito, N. Oshima, N. Kitamura, S. Ishizaka, Y. Hinatsu, M. Wakeshima, M. Kato, K. Tsuge, M. Sawamura, *J. Am. Chem. Soc.* **2008**, *130*, 10044.
[5] T. Lasanta, M. E. Olmos, A. Laguna, J. M. López-de-Luzuriaga, P. Naumov, *J. Am. Chem. Soc.* **2011**, *133*, 16358.
[6] S. Mizukami, H. Houjou, K. Sugaya, E. Koyama, H. Tokuhisa, T. Sasaki, M. Kanesato, *Chem. Mater.* **2005**, *17*, 50.
[7] V. N. Kozhevnikov, B. Donnio, D. W. Bruce, *Angew. Chem. Int. Ed.* **2008**, *47*, 6286.
[8] H. Bi, D. Chen, D. Li, Y. Yuan, D. Xia, Z. Zhang, H. Zhang, Y. Wang, *Chem. Commun.* **2011**, *47*, 4135.
[9] A. L. Balch, *Angew. Chem. Int. Ed.* **2009**, *48*, 2641.
[10] G. Zhang, J. Lu, M. Sabat, C. L. Fraser, *J. Am. Chem. Soc.* **2010**, *132*, 2160.
[11] Y. Sagara, T. Mutai, I. Yoshikawa, K. Araki, *J. Am. Chem. Soc.* **2007**, *129*, 1520.
[12] Y. Sagara, T. Kato, *Angew. Chem. Int. Ed.* **2008**, *47*, 5175.
[13] Z. Zhang, D. Yao, T. Zhou, H. Zhang, Y. Wang, *Chem. Commun.* **2011**, *47*, 7782.
[14] Y. Dong, B. Xu, J. Zhang, X. Tan, L. Wang, J. Chen, H. Lv, S. Wen, B. Li, L. Ye, B. Zou, W. Tian, *Angew. Chem. Int. Ed.* **2012**, *51*, 10782.
[15] J. Kunzelman, M. Kinami, B. R. Crenshaw, J. D. Protasiewicz, C. Weder, *Adv. Mater.* **2008**, *20*, 119.
[16] S.-J. Yoon, J. W. Chung, J. Gierschner, K. S. Kim, M.-G. Choi, D. Kim, S. Y. Park, *J. Am. Chem. Soc.* **2010**, *132*, 13675.
[17] X. Luo, J. Li, C. Li, L. Heng, Y. Q. Dong, Z. Liu, Z. Bo, B. Z. Tang, *Adv. Mater.* **2011**, *23*, 3261.
[18] J. Wang, J. Mei, R. Hu, J. Z. Sun, A. Qin, B. Z. Tang, *J. Am. Chem. Soc.* **2012**, *134*, 9956.
[19] N. Mizoshita, T. Tani, S. Inagaki, *Adv. Mater.* **2012**, *24*, 3350.
[20] M.-J. Teng, X.-R. Jia, S. Yang, X.-F. Chen, Y. Wei, *Adv. Mater.* **2012**, *24*, 1255.
[21] Y. Ren, W. H. Kan, M. A. Henderson, P. G. Bomben, C. P. Berlinguette, V. Thangadurai, T. Baumgartner, *J. Am. Chem. Soc.* **2011**, *133*, 17014.
[22] S. Tsuzuki, H. Tokuda, K. Hayamizu, M. Watanabe, *J. Phys. Chem. B* **2005**, *109*, 16474.
[23] K. Fumino, A. Wulf, R. Ludwig, *Angew. Chem. Int. Ed.* **2008**, *47*, 3830.
[24] K. Fumino, A. Wulf, S. P. Verevkin, A. Heintz, R. Ludwig, *ChemPhysChem* **2010**, *11*, 1623.
[25] S. Wei, X.-G. Wei, X. Su, J. You, Y. Ren, *Chem. Eur. J.* **2011**, *17*, 5965.
[26] A. Paul, P. K. Mandal, A. Samanta, *J. Phys. Chem. B* **2005**, *109*, 9148.
[27] S. Ahrens, A. Peritz, T. Strassner, *Angew. Chem. Int. Ed.* **2009**, *48*, 7908.
[28] L. Zhu, G. Li, L. Luo, P. Guo, J. Lan, J. You, *J. Org. Chem.* **2009**, *74*, 2200.
[29] J. D. Holbrey, W. M. Reichert, R. D. Rogers, *J. Chem. Soc., Dalton Trans.* **2004**, 2267.

© 2013 WILEY-VCH Verlag GmbH & Co. KGaA, Weinheim